Mossy fiber Zn^{2+} spillover modulates heterosynaptic *N*-methyl-D-aspartate receptor activity in hippocampal CA3 circuits

Sayaka Ueno,[1] Masako Tsukamoto,[1] Tomoya Hirano,[2] Kazuya Kikuchi,[2] Maki K. Yamada,[1] Nobuyoshi Nishiyama,[1] Tetsuo Nagano,[2] Norio Matsuki,[1] and Yuji Ikegaya[1]

[1]Laboratory of Chemical Pharmacology and [2]Laboratory of Bioorganic and Medicinal Chemistry, Graduate School of Pharmaceutical Sciences, The University of Tokyo, Tokyo 113-0033, Japan

Although Zn^{2+} is contained in large amounts in the synaptic terminals of hippocampal mossy fibers (MFs), its physiological role in synaptic transmission is poorly understood. By using the newly developed high-sensitivity Zn^{2+} indicator ZnAF-2, the spatiotemporal dynamics of Zn^{2+} was monitored in rat hippocampal slices. When high-frequency stimulation was delivered to the MFs, the concentration of extracellular Zn^{2+} was immediately elevated in the stratum lucidum, followed by a mild increase in the stratum radiatum adjacent to the stratum lucidum, but not in the distal area of stratum radiatum. The Zn^{2+} increase was insensitive to a non–*N*-methyl-D-aspartate (NMDA) receptor antagonist but was efficiently attenuated by tetrodotoxin or Ca^{2+}-free medium, suggesting that Zn^{2+} is released by MF synaptic terminals in an activity-dependent manner, and thereafter diffuses extracellularly into the neighboring stratum radiatum. Electrophysiological analyses revealed that NMDA receptor–mediated synaptic responses in CA3 proximal stratum radiatum were inhibited in the immediate aftermath of MF activation and that this inhibition was no longer observed in the presence of a Zn^{2+}-chelating agent. Thus, Zn^{2+} serves as a spatiotemporal mediator in imprinting the history of MF activity in contiguous hippocampal networks. We predict herein a novel form of metaplasticity, i.e., an experience-dependent non-Hebbian modulation of synaptic plasticity.

Introduction

Zn^{2+}, one of the most abundant divalent metal ions in the central nervous system (CNS),* is mainly stored in the synaptic vesicles of excitatory synapses, particularly the synaptic terminals of hippocampal mossy fibers (MFs), and is coreleased with neurotransmitters in response to synaptic activity (Assaf and Chung, 1984; Howell et al., 1984). Zn^{2+} is known to modulate postsynaptic neurotransmitter receptor activity. For instance, it inhibits *N*-methyl-d-aspartate (NMDA) receptors (Peters et al., 1987) and γ-aminobutyric acid receptors (Westbrook and Mayer, 1987), and potentiates α-amino-3-hydroxy-5-methyl-4-isoxazoleproprionic acid (AMPA) receptors (Rassendren et al., 1990). Zn^{2+} is also able to permeate ligand-gated channels, e.g., NMDA receptor channels, Ca^{2+}-permeable AMPA/kainate receptor channels, and voltage-dependent Ca^{2+} channels (Li et al., 2001b), and may influence various intracellular signaling pathways (Brewer et al., 1979; Hubbard et al., 1991; Shumilla et al., 1998; Park and Koh, 1999; Eom et al., 2001). In addition to its neuromodulatory roles, a marked increase in intracellular Zn^{2+} causes neuronal death under pathological conditions such as brain ischemia (Tonder et al., 1990; Koh et al., 1996; Choi and Koh, 1998) and epileptic seizures (Lee et al., 2000).

Despite numerous studies on Zn^{2+} action in the CNS, the physiological significance of synaptically released Zn^{2+} is largely unknown, one reason being that the spatiotemporal Zn^{2+} dynamics during synaptic activity remains unclear to date. To explore Zn^{2+} behavior, most of the previous studies have utilized such fluorescent Zn^{2+} indicators as Newport Green (Li et al., 2001b) and Mag-Fura-5 (Sensi et al., 1997; Canzoniero et al., 1999). These indicators have relatively low affinity for Zn^{2+}, their K_d values being 1 and 27 nM, respectively. Considering that a very low concentration of extracellular Zn^{2+} ($[Zn^{2+}]_o$) is sufficient to inhibit the activity of NR2A-containing NMDA receptors, the major receptor form in the mature hippocampus (IC_{50} = ~5 nM) (Paoletti

et al., 1997), such low-sensitivity indicators cannot trace Zn^{2+} dynamics at a low but physiologically significant level. In addition, these indicators exhibit low selectivity for Zn^{2+} in the presence of other ions; e.g., Mag-Fura-5 shows affinity for Ca^{2+} and Mg^{2+} as well. Another problem is that Newport green shows high background fluorescence even in the absence of Zn^{2+}, and a relatively small increase in fluorescence intensity after exposure to Zn^{2+}. To overcome these problems, we employ ZnAF-2, a novel fluorescent indicator, to monitor Zn^{2+} dynamics. ZnAF-2 has a low K_d value of 2.7 nM for Zn^{2+} and its fluorescence is minimally changed in the presence of Ca^{2+}, Mg^{2+}, Cd^{2+}, Ni^{2+}, or other heavy metal ions (Hirano et al., 2000). Also, ZnAF-2 has no apparent toxicity to living cells (Hirano et al., 2000; 2002). These features allow us to assess physiologically relevant Zn^{2+} behavior in hippocampal slices without interference from other heavy metal ions.

Here we report that Zn^{2+} is released by MF synaptic terminals in an activity-dependent manner and diffuses extracellularly into the adjacent stratum radiatum after tens of seconds, thereby inhibiting NMDA receptor–mediated synaptic responses. Thus, the synaptically released Zn^{2+} may act as an activity-dependent, heterosynaptic modulator of hippocampal synaptic transmission.

Results and discussion

We first confirmed the intracellular localization of endogenous Zn^{2+} in hippocampal slices by using ZnAF-2-DA, a membrane-permeable, diacetylated form of ZnAF-2. The spatial distribution of ZnAF-2 fluorescence closely resembles to Timm's stain, a classical histochemical technique to detect Zn^{2+} (Ikegaya et al., 2000); the signal was evident in dentate hilus, stratum lucidum, and a small part of CA3 stratum oriens (Fig. 1, A and B). The ZnAF-2 fluorescence was almost completely eliminated 15 min after bath application of 25 μM N,N,N',N'-tetrakis(2-pyridylmethyl)ethylenediamine (TPEN), a membrane-permeable Zn^{2+} chelator (Fig. 1, C and D). These results indicate that ZnAF-2 successfully detects endogenous Zn^{2+} of MF synaptic terminals in living hippocampal slices.

To examine the spatiotemporal dynamics of extracellular Zn^{2+} after synaptic activity, slices were submerged in membrane-impermeable ZnAF-2, and electrical stimulation was applied to the MFs (Fig. 2 A). When the MFs were trained at 100 Hz for 2 s, $[Zn^{2+}]_o$ in stratum lucidum immediately increased, peaking within 5 s (Figs. 2, B and C, and 3 A). In the stratum radiatum proximal to stratum lucidum (<100 μm from stratum lucidum) and stratum pyramidale, $[Zn^{2+}]_o$ gradually increased and reached a peak about 15 s after MF tetanization (Figs. 2, B and C, and 3 A). Thereafter, the ZnAF-2 signal slightly declined but did not come back to baseline at least during a 600-s observation period. When 25 μM TPEN was added 120 s after the MF tetanization, the fluorescence was rapidly quenched ($n = 3$, unpublished data), which suggests that the sustained ZnAF-2 signal is due to a relatively slow clearance of released Zn^{2+}. A change in $[Zn^{2+}]_o$ was minimally observed in the distal area of stratum radiatum (>200 μm far from stratum lucidum) (Figs. 2, B and C and 3 A). The data indicate an intriguing
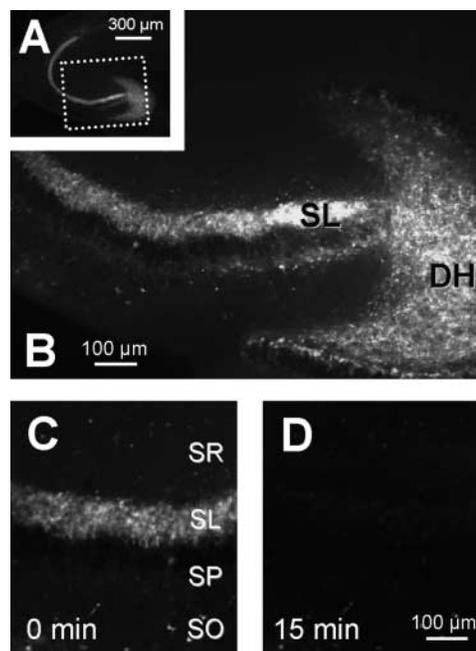

Figure 1. **ZnAF-2 labels endogenous Zn^{2+} in rat hippocampal slices.** (A) Confocal image of a hippocampal slice loaded with a membrane-permeable, diacetylated form of ZnAF-2. (B) Confocal image of the boxed region in *A* taken at higher magnification. The fluorescent signal of ZnAF-2 was detected in subgranular zone, dentate hilus (*DH*), stratum lucidum (*SL*) and a small portion of stratum oriens (*SO*) but not seen in stratum radiatum (*SR*) or stratum pyramidale (*SP*), which corresponds to intracellular Zn^{2+} localization. ZnAF-2 images of the CA3 area in a hippocampal slice were obtained immediately before (C) and 15 min (D) after bath application of 25 μM TPEN. ZnAF-2 signal was eliminated by Zn^{2+} chelation by TPEN.

possibility that Zn^{2+} present in MF terminals are not only released into synaptic clefts but also subsequently diffuses into the neighboring area. Importantly, photobleaching of the proximal area of stratum radiatum in the continuous presence of exogenous Zn^{2+} (200 μM) was followed by no apparent recovery of fluorescent signal within at least 60 s (Fig. 2 D), suggesting that unbleached fluorophore cannot diffuse from stratum lucidum into the adjacent stratum radiatum. Therefore, the increase in ZnAF-2 fluorescence intensity in stratum radiatum after MF stimulation is unlikely due to a diffusion of Zn^{2+}–ZnAF-2 complexes, but rather does reflect the distribution of Zn^{2+} itself.

MF-activated $[Zn^{2+}]_o$ increases in stratum lucidum and radiatum were both abolished by the Na^+ channel blocker tetrodotoxin (2 μM) or extracellular Ca^{2+} removal (Fig. 2 E). Thus, the release of Zn^{2+} is dependent on neural activity and Ca^{2+}-dependent vesicular release. The non-NMDA receptor antagonist 6-cyano-7-nitroquinoxaline-2,3-dione (CNQX) (20 μM) was virtually ineffective against the $[Zn^{2+}]_o$ elevation (Fig. 2 E). Therefore, postsynaptic activation is not indispensable for the $[Zn^{2+}]_o$ dynamics after MF activation. This result also suggests no contribution of a possible Zn^{2+} release from the apical dendrites of CA3 pyramidal cells via postsynaptic depolarization or from synapses of CA3 recurrent circuits via disynaptic activation. Taken together, our findings indicate that Zn^{2+} is released from MF terminals in response to MF activity, and that afterward it
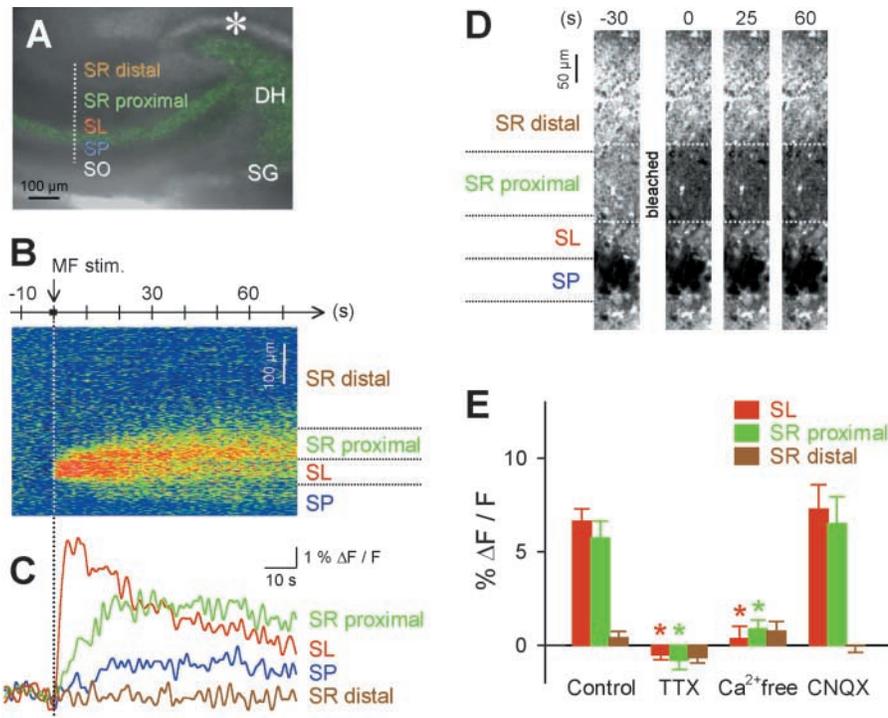
Figure 2. **Extracellular Zn²⁺ release and diffusion after MF activation.** (A) An image of the dentato-CA3 area of a hippocampal slice perfused with ZnAF-2. Confocal ZnAF-2 signal is shown as a green-colorized scale, superimposed on a transmitted beam image. Bipolar electrodes (∗) were placed in stratum granulosum (*SG*) to stimulate the MFs. The dotted line marks the transect of illumination during line-scan imaging. (B) Line-scan image of ZnAF-2 taken at the points indicated in *A*. The temporal resolution was 1 s per line. "*Hotter*" colors correspond to increased $[Zn^{2+}]_o$ on an arbitrary pseudo-color scale. (C) Data extracted from the image in *B*, along the time axis. Each point in time is the average %ΔF/F value across the spatial axis of the region separated by the horizontal dotted lines in B, i.e., the stratum radiatum far from stratum lucidum (SR distal, brown), the stratum radiatum near stratum lucidum (SR proximal, green), stratum lucidum (SL, red) and stratum pyramidale (SP, blue). The MFs were tetanized at 100 Hz for 2 s (MF stim.) at the time indicated by the vertical dotted line. MF stimulation elicited an immediate increase in $[Zn^{2+}]_o$ in stratum lucidum, and a slow increase in stratum pyramidale and proximal stratum radiatum but no apparent change in distal stratum radiatum. *D*, The area between the white dotted lines (a 0.02 mm² square) was strongly illuminated in the presence of 200 μM Zn²⁺ for photobleaching and imaged 30 s before and 0, 25 and 60 s after the illumination. Fluorescence recovery owing to a diffusion of Zn²⁺-ZnAF-2 complex was not found within at least 60 s. *E*, Summary data of %ΔF/F 15 s after MF stimulation in stratum lucidum (red) and proximal (green) and distal (brown) stratum radiatum in the absence (Control) or presence of 2 μM tetrodotoxin (*TTX*) or 20 μM CNQX, or in Ca²⁺-free medium. *P < 0.01 versus Control; Student's *t* test. Data are means ± SEM of 5–13 slices.

diffuses into adjacent stratum radiatum even though it cannot reach the distal region.

To determine how the frequency of MF activity affects the spatiotemporal dynamics of synaptically released Zn²⁺, the MFs were activated by repetitive stimulation at 1 or 5 Hz. In either case, an apparent increase in $[Zn^{2+}]_o$ was observed in stratum lucidum and proximal stratum radiatum, but the peak $[Zn^{2+}]_o$ was smaller and the kinetics was slower as compared with those induced by a 100 Hz tetanus (Fig. 3, B and C). The time course of the $[Zn^{2+}]_o$ changes was almost equivalent in both the subregions (Fig. 3, B and C). No MF stimulation induced no change of $[Zn^{2+}]_o$ (Fig. 3 D).

Previous studies indicated that Zn²⁺ inhibits NMDA receptor function at very low concentrations (Paoletti et al., 1997). Zn²⁺ spread to stratum radiatum is, therefore, possible to modulate NMDA receptor function therein. To address the functional significance of Zn²⁺ spillover from MF synapses, NMDA receptor–mediated field excitatory postsynaptic potential (fEPSP_NMDA) were extracellularly recorded at associational/commissural-CA3 pyramidal cell synapses. When a recording electrode was positioned in the proximal region of stratum radiatum (<100 μm from stratum lucidum), fEPSP_NMDA declined transiently in response to MF tetanization (100 Hz for 2 s); the inhibition reached an apparent peak after 15 s and rapidly returned to baseline by 60 s (Fig. 4). This depression was completely relieved 15 min after bath application of 25 μM TPEN (Fig. 4 B), whereas TPEN alone did not affect baseline fEPSP_NMDA (*n* = 7; P > 0.1; paired *t* test; unpublished data). The data

indicate that endogenous Zn²⁺ mediates fEPSP_NMDA-blocking action of MF tetanization but does not significantly work under basal conditions. As expected from the results of ZnAF-2, fEPSP_NMDA recorded from the distal part of stratum radiatum (>200 μm far from stratum lucidum) was insensitive to the same stimulation of the MFs (Fig. 4).

Finally, we examined AMPA receptor function. The MF stimulation failed to affect fEPSP_AMPA recorded from proximal stratum radiatum (Fig. 4 B). The data suggests that AMPA receptors are not a target of endogenous Zn²⁺ and also that under our experimental conditions, the associational/commissural synaptic responses are completely separated from MF synaptic component, which is further supported by a observation that neither fEPSP_AMPA nor fEPSP_NMDA was affected by application of the group II metabotropic glutamate receptor agonist DCG-IV (1 μM), which can selectively inhibit glutamate release from MF synapses without affecting associational/commissural synapses (Kamiya et al., 1996) (*n* = each four slices; P > 0.1; paired *t* test). Taken together, mossy fiber Zn²⁺ selectively alters NMDA receptor function in the vicinity of MF synapses. These data suggest that MF activity transiently produces a gradient inhibition of NMDA receptor function along the apical dendrite of a CA3 pyramidal cell.

Although the role of Zn²⁺ in MF terminals has been unclear, the development of the high-affinity, Zn²⁺-specific indicator ZnAF-2 has enabled us to precisely map the extracellular fate of synaptically released Zn²⁺. We have shown for the first time that Zn²⁺ released from MF terminals is dis-
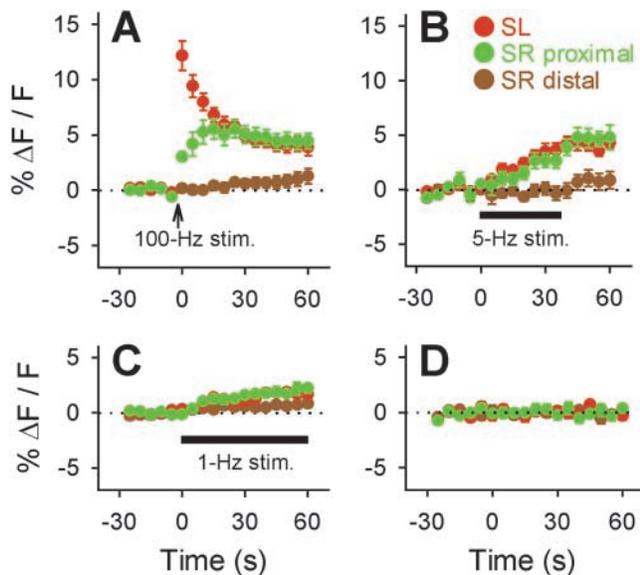
Figure 3.   **Frequency-dependent dynamics of synaptically released Zn²⁺.** (A–C) Time course of %ΔF/F of ZnAF-2 in stratum lucidum (SL, red), proximal stratum radiatum (SR proximal, green) and distal stratum radiatum (SR distal, brown) after MF stimulation of 200 pulses at 100 Hz (A), 200 pulses 5 Hz (B) and 60 pulses at 1 Hz (C). The stimulation was applied from time 0. While the 100 Hz stimulation evoked a rapid, large increase in [Zn²⁺]ₒ, the lower frequencies of stimulation caused a slow, moderate increase. (D) Basal ΔF/F (no MF stimulation) was stable. Data represent means ± SEM of 5–13 slices.

Figure 4.   **Zn²⁺-mediated, heterosynaptic inhibition of NMDA receptors in stratum radiatum after MF activation.** (A) fEPSP$_{NMDA}$ in associational/commissural fiber-CA3 pyramidal cell synapses were extracellularly recorded from the stratum radiatum proximal to (closed circles) or far from (open circles) stratum lucidum in Mg²⁺-free solution containing 20 μM CNQX. When MF stimulation (100 Hz for 2 s) was applied at time from −2 to 0 (MF stim.), the NMDA component was temporarily depressed. Representative traces of fEPSP$_{NMDA}$ at times −5 and 15 are shown in the insets. (B) Summary data for the effect of MF stimulation on AMPA and NMDA responses in proximal and distal stratum radiatum (SR). The ordinate indicates an average change in fEPSPs 15 s after MF stimulation (100 Hz for 2 s). The fEPSP$_{NMDA}$ depression was blocked by 25 μM TPEN. Neither fEPSP$_{AMPA}$ in proximal stratum radiatum nor fEPSP$_{NMDA}$ in distal |stratum radiatum was unaffected by MF activation. *P < 0.01; Student's t test. Data are means ± SEM of 5–7 slices.

tributed over the surrounding areas (up to ~100 μm far from the released site) within tens of seconds, and also that the Zn²⁺ spillover causes a heterosynaptic inhibition of NMDA receptor function. Therefore, Zn²⁺ is likely to serve as an intersynaptic mediator in etching the history of MF activity into neighboring synapses in hippocampal circuits.

Recent evidence showed that Zn²⁺ plays a role in synaptic transmission and plasticity at MF-CA3 synapses. The baseline level of Zn²⁺ yields a tonic inhibition of NMDA receptors at MF synapses, and MF tetanization results in a further inhibition by bulk release of Zn²⁺ (Vogt et al., 2000). The endogenous Zn²⁺ may also be involved in the induction of NMDA receptor–independent long-term potentiation at MF synapses (Weiss et al., 1989; Lu et al., 2000; Vogt et al., 2000; Li et al., 2001a), in which Zn²⁺ may behave like a second messenger after entering into presynaptic or postsynaptic neurons (Li et al., 2001a). Thus, past studies on mossy fiber Zn²⁺ have focused mainly on its homosynaptic action. However, if Zn²⁺ could only coact with neurotransmitters at the released site, the role of Zn²⁺ would be limited to a monotonous modulation. Here we found that Zn²⁺ influences NMDA receptor function even at neighboring synapses in stratum radiatum as well. Similarly, Zn²⁺ probably exerts its heterosynaptic action at adjacent MF synapses in stratum lucidum. Therefore, we consider that this metal ion is assigned a highly dynamic role in regulating the physiological function of hippocampal CA3 local circuits.

Zn²⁺ is shown to inhibit NMDA currents and potentiate AMPA currents (Rassendren et al., 1990), but we found no evidence that fEPSP$_{AMPA}$ was increased after MF activation. Some reports indicated that AMPA receptors have different subunit compositions including splicing variants, thereby
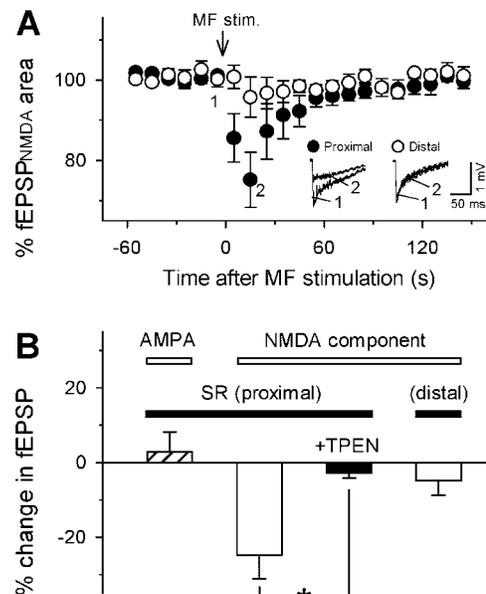
showing different responsiveness to Zn²⁺ (Dreixler and Leonard, 1994; Shen and Yang, 1999). Indeed, only half of the CA3 neurons are sensitive to Zn²⁺ (Lin et al., 2001). This may account for no change in AMPA responses in our experiments. However, a more plausible explanation is a difference in the Zn²⁺ sensitivity of NMDA and AMPA receptors. The concentrations giving a half-maximal response are ~5 nM for NMDA receptors (Paoletti et al., 1997) and 30 μM for AMPA receptors (Rassendren et al., 1990); AMPA receptors are nearly 10⁴-fold less sensitive to Zn²⁺. The peak [Zn²⁺]ₒ in stratum radiatum may be in the range of 5–30 μM.

There was an apparent discrepancy in time course between the increase of ZnAF-2 signal and the inhibition of fEPSP$_{NMDA}$ in stratum radiatum. Both peaked about 15 s after MF stimulation. However, after the peak, ZnAF-2 signal was kept high for >60 s while fEPSP$_{NMDA}$ returned to baseline within 60 s. Because of the high-affinity of ZnAF-2 (K_d = 2.7 nM), the indicator may interfere with intrinsic Zn²⁺ uptake system, and Zn²⁺ may remain in the extracellular space as a stable complex with ZnAF-2. Therefore, we cannot exclude the possibility that ZnAF-2 signal does not strictly reflect naturally occurring Zn²⁺ dynamics, particularly in the decay kinetics. Nonetheless, this does not disclaim the fact that Zn²⁺ diffuses from the released site. The result of ZnAF-2 photobleaching and the TPEN effect on

$fEPSP_{NMDA}$ provide unambiguous evidence for a significant spread of Zn^{2+} beyond the MF region.

In conclusion, the present study has established that the metal ion Zn^{2+} is an activity-dependent, spatiotemporal modulator of NMDA receptor function in hippocampal CA3 local circuits and that the extracellular Zn^{2+} gradient made after MF activation reaches $\sim$100 μm but eliminates within tens of seconds. The spillover range is probably variable along with MF presynaptic release probability, which is known to increase after the induction of long-term potentiation (Toth et al., 2000). Considering that NMDA receptors serve as a coincidence detector in synaptic plasticity and learning and memory (Bliss and Collingridge, 1993; Martin et al., 2000), the Zn^{2+} gradient may yield different learning rules along the apical dendrite of a CA3 pyramidal cell, and therefore MF activation may emphasize a difference in information processing between the distal and proximal segments of the postsynaptic dendrite. This work predicts a novel form of experience-dependent modulation of synaptic plasticity, i.e., Zn^{2+}-mediated, heterosynaptic metaplasticity, and thus provides new insights into information processing of the hippocampus.

Materials and methods

Materials
ZnAF-2 was chemically synthesized and purified as described previously (Hirano et al., 2000). D-2-amino-5-phosphonopentanoic acid, CNQX, and tetrodotoxin were purchased from Sigma-Aldrich. $ZnCl_2$ and TPEN were obtained from Dojindo. DCG-IV was obtained from Tocris.

Hippocampal slice preparation
Postnatal 17–27-d-old Wistar/ST rats (SLC) were anesthetized with ether and decapitated, according to the Japanese Pharmacological Society guide for the care and use of laboratory animals. The brain was quickly removed and immersed in ice-cold artificial cerebrospinal fluid (ACSF) containing 124 mM NaCl, 25 mM NaHCO$_3$, 3 mM KCl, 1.24 mM KH$_2$PO$_4$, 1.4 mM MgSO$_4$, 2.2 mM CaCl$_2$, and 10 mM glucose, continuously bubbled with 95% O$_2$ and 5% CO$_2$. Horizontal hippocampal slices of 300–350 μm in thickness were prepared using the vibratome ZERO-1 (Dosaka).

Extracellular Zn^{2+} imaging
ZnAF-2 is incapable of permeating the cell membrane, but its diacetylated form can be passively loaded into cells where it is cleaved to cell-impermeant products by intracellular acetylase (Hirano et al., 2000). Therefore, for intracellular Zn^{2+} fluorescence imaging, hippocampal slices were preloaded with 10 μM ZnAF-2 diacetate (ZnAF-2-DA) in the dark for 90 min at room temperature, and washed with ACSF for at least 30 min to remove unincorporated ZnAF-2-DA from the intercellular space. For extracellular Zn^{2+} detection, slices were loaded with 10 μM ZnAF-2 for at least 90 min. Zn^{2+} imaging was performed at 27–32°C with the confocal microscopic system BioRad MRC-1000 equipped with the inverted microscope ECLIPSE TE300 (Nikon) and an argon ion laser (monochromator set to 492 nm). Emitted light images at 514 nm or greater were acquired at rates of 0.2-1 Hz through a 10× objective (0.45 of numerical aperture) with an intensified CCD camera and digitized with Laser Sharp Acquisition (Bio-Rad Laboratories). Autofluorescence was below the detection limits of the camera, and photobleaching was negligible under these conditions; neither was subtracted from the data.

Electrical stimulation and extracellular recording
To induce the release of Zn^{2+} from MF terminals, bipolar tungsten electrodes were placed in the stratum granulosum of the dentate gyrus, and trains of stimuli (at 1, 5, or 100 Hz, each rectangular pulse with a 60-μs duration and 500-μA intensity) were delivered. For extracellular recording, slices were preincubated in a 95% O$_2$–5% CO$_2$-saturated ACSF for at least 1 h at 32°C, placed in an interface recording chamber, and perfused with ACSF equilibrated with 95% O$_2$ and 5% CO$_2$ at 32°C. Test stimuli were delivered every 10 s through the bipolar tungsten electrodes positioned across the associational/commissural fibers in the middle part of CA3 stratum radiatum. The fEPSPs were recorded from CA3 stratum radiatum by a glass microelectrode filled with 0.15 M NaCl ($\sim$1 MΩ of resistance). To check whether the fEPSPs were contaminated with MF responses, single-pulse stimulation was applied to the MFs. We could easily confirm that this stimulation induced a positive field response in stratum radiatum if we obtained a complete separation of the two inputs. When the MF stimulation evoked a negative response like associational/commissural stimulation, the experiment was discarded. AMPA receptor–mediated response ($fEPSP_{AMPA}$) was recorded in the presence of 50 μM D-2-amino-5-phosphonopentanoic acid and evaluated by its amplitude. $fEPSP_{NMDA}$ was isolated in Mg^{2+}-free ACSF containing 20 μM CNQX and evaluated by the area under the curve from 4 to 45 ms after test stimulus. The stimulus intensity was set to produce $fEPSP_{AMPA}$ with an amplitude of 50% of maximum or $fEPSP_{NMDA}$ with an area of 70% of maximum. The baseline was recorded for at least 10 min to ensure the stability of the response.

References

Assaf, S.Y., and S.H. Chung. 1984. Release of endogenous Zn^{2+} from brain tissue during activity. *Nature.* 308:734–736.

Bliss, T.V., and G.L. Collingridge. 1993. A synaptic model of memory: long-term potentiation in the hippocampus. *Nature.* 361:31–39.

Brewer, G.J., J.C. Aster, C.A. Knutsen, and W.C. Kruckeberg. 1979. Zinc inhibition of calmodulin: a proposed molecular mechanism of zinc action on cellular functions. *Am. J. Hematol.* 7:53–60.

Canzoniero, L.M., D.M. Turetsky, and D.W. Choi. 1999. Measurement of intracellular free zinc concentrations accompanying zinc-induced neuronal death. *J. Neurosci.* 19:RC31.

Choi, D.W., and J.Y. Koh. 1998. Zinc and brain injury. *Annu. Rev. Neurosci.* 21: 347–375.

Dreixler, J.C., and J.P. Leonard. 1994. Subunit-specific enhancement of glutamate receptor responses by zinc. *Mol. Brain Res.* 22:144–150.

Eom, S.J., E.Y. Kim, J.E. Lee, H.J. Kang, J. Shim, S.U. Kim, B.J. Gwag, and E.J. Choi. 2001. Zn^{2+} induces stimulation of the c-Jun N-terminal kinase signaling pathway through phosphoinositide 3-kinase. *Mol. Pharmacol.* 59:981–986.

Hirano, T., K. Kikuchi, Y. Urano, T. Higuchi, and T. Nagano. 2000. Highly zinc-selective fluorescent sensor molecules suitable for biological applications. *J. Am. Chem. Soc.* 122:12399–12400.

Hirano, T., K. Kikuchi, Y. Urano, T. Higuchi, and T. Nagano. 2002. Improvement and biological applications of fluorescent probes for zinc, ZnAFs. *J. Am. Chem. Soc.* In press.

Howell, G.A., M.G. Welch, and C.J. Frederickson. 1984. Stimulation-induced uptake and release of zinc in hippocampal slices. *Nature.* 308:736–738.

Hubbard, S.R., W.R. Bishop, P. Kirschmeier, S.J. George, S.P. Cramer, and W.A. Hendrickson. 1991. Identification and characterization of zinc binding sites in protein kinase C. *Science.* 254:1776–1779.

Ikegaya, Y., N. Nishiyama, and N. Matsuki. 2000. L-type Ca^{2+} channel blocker inhibits mossy fiber sprouting and cognitive deficits following pilocarpine seizures in immature mice. *Neuroscience.* 98:647–659.

Kamiya, H., H. Shinozaki, and C. Yamamoto. 1996. Activation of metabotropic glutamate receptor type 2/3 suppresses transmission at rat hippocampal mossy fibre synapses. *J. Physiol.* 493:447–455.

Koh, J.Y., S.W. Suh, B.J. Gwag, Y.Y. He, C.Y. Hsu, and D.W. Choi. 1996. The role of zinc in selective neuronal death after transient global cerebral ischemia. *Science.* 272:1013–1016.

Lee, J.Y., T.B. Cole, R.D. Palmiter, and J.Y. Koh. 2000. Accumulation of zinc in degenerating hippocampal neurons of ZnT3-null mice after seizures: evidence against synaptic vesicle origin. *J. Neurosci.* 20:RC79.

Li, Y., C.J. Hough, C.J. Frederickson, and J.M. Sarvey. 2001a. Induction of mossy fiber → Ca3 long-term potentiation requires translocation of synaptically released Zn^{2+}. *J. Neurosci.* 21:8015–8025.

Li, Y., C.J. Hough, S.W. Suh, J.M. Sarvey, and C.J. Frederickson. 2001b. Rapid translocation of Zn^{2+} from presynaptic terminals into postsynaptic hippocam-

pal neurons after physiological stimulation. *J. Neurophysiol.* 86:2597–2604.

Lin, D.D., A.S. Cohen, and D.A. Coulter. 2001. Zinc-induced augmentation of excitatory synaptic currents and glutamate receptor responses in hippocampal CA3 neurons. *J. Neurophysiol.* 85:1185–1196.

Lu, Y.M., F.A. Taverna, R. Tu, C.A. Ackerley, Y.T. Wang, and J. Roder. 2000. Endogenous Zn^{2+} is required for the induction of long-term potentiation at rat hippocampal mossy fiber-CA3 synapses. *Synapse.* 38:187–197.

Martin, S.J., P.D. Grimwood, and R.G. Morris. 2000. Synaptic plasticity and memory: an evaluation of the hypothesis. *Annu. Rev. Neurosci.* 23:649–711.

Park, J.A., and J.Y. Koh. 1999. Induction of an immediate early gene egr-1 by zinc through extracellular signal-regulated kinase activation in cortical culture: its role in zinc-induced neuronal death. *J. Neurochem.* 73:450–456.

Peters, S., J. Koh, and D.W. Choi. 1987. Zinc selectively blocks the action of *N*-methyl-d-aspartate on cortical neurons. *Science.* 236:589–593.

Paoletti, P., P. Ascher, and J. Neyton. 1997. High-affinity zinc inhibition of NMDA NR1-NR2A receptors. *J. Neurosci.* 17:5711–5725.

Rassendren, F.A., P. Lory, J.P. Pin, and J. Nargeot. 1990. Zinc has opposite effects on NMDA and non-NMDA receptors expressed in *Xenopus* oocytes. *Neuron* 4:733–740.

Sensi, S.L., L.M. Canzoniero, S.P. Yu, H.S. Ying, J.Y. Koh, G.A. Kerchner, and D.W. Choi. 1997. Measurement of intracellular free zinc in living cortical neurons: routes of entry. *J. Neurosci.* 17:9554–9564.

Shen, Y., and X.L. Yang. 1999. Zinc modulation of AMPA receptors may be relevant to splice variants in carp retina. *Neurosci. Lett.* 259:177–180.

Shumilla, J.A., K.E. Wetterhahn, and A. Barchowsky. 1998. Inhibition of NF-kappa B binding to DNA by chromium, cadmium, mercury, zinc, and arsenite in vitro: evidence of a thiol mechanism. *Arch. Biochem. Biophys.* 349:356–362.

Tonder, N., F.F. Johansen, C.J. Frederickson, J. Zimmer, and N.H. Diemer. 1990. Possible role of zinc in the selective degeneration of dentate hilar neurons after cerebral ischemia in the adult rat. *Neurosci. Lett.* 109:247–252.

Toth, K., G. Suares, J.J. Lawrence, E. Philips-Tansey, and C.J. McBain. 2000. Differential mechanisms of transmission at three types of mossy fiber synapse. *J. Neurosci.* 20:8279–8289.

Vogt, K., J. Mellor, G. Tong, and R. Nicoll. 2000. The actions of synaptically released zinc at hippocampal mossy fiber synapses. *Neuron.* 26:187–196.

Weiss, J.H., J.Y. Koh, C.W. Christine, and D.W. Choi. 1989. Zinc and LTP. *Nature.* 338:212.

Westbrook, G.L., and M.L. Mayer. 1987. Micromolar concentrations of Zn^{2+} antagonize NMDA and GABA responses of hippocampal neurons. *Nature.* 328:640–643.